

Exclusive Double-Charmonium Production from e^+e^- Annihilation into a Virtual Photon

Eric Braaten

Physics Department, Ohio State University, Columbus, Ohio 43210 and

*Fermi National Accelerator Laboratory,
P. O. Box 500, Batavia, Illinois 60510*

Jungil Lee

Department of Physics, Korea University, Seoul 136-701, Korea

(Dated: November 5, 2018)

Abstract

We calculate the exclusive cross sections for e^+e^- annihilation into two charmonium states through a virtual photon. Purely electromagnetic contributions are surprisingly large, changing the cross sections by as much as 21%. The predicted cross section for $J/\psi + \eta_c$ is about an order of magnitude smaller than a recent measurement by the BELLE Collaboration, although part of the discrepancy can be attributed to large relativistic corrections. The cross sections for S -wave + P -wave, P -wave + P -wave, and S -wave + D -wave charmonium states are also calculated. It may be possible to discover the D -wave state $\eta_{c2}(1D)$ at the B factories through the mode $J/\psi + \eta_{c2}$, whose cross section is predicted to be about a factor of 10 smaller than $J/\psi + \eta_c$.

PACS numbers: 12.38.-t, 12.38.Bx, 13.20.Gd, 14.40.Gx

I. INTRODUCTION

NRQCD factorization is a systematic framework for calculating the inclusive cross sections for producing heavy quarkonium [1]. The cross section for a charmonium state is expressed as the sum over $c\bar{c}$ channels of products of perturbative $c\bar{c}$ cross section and nonperturbative NRQCD matrix elements. The relative importance of the various terms in the factorization formula is determined by the order in α_s of the $c\bar{c}$ cross section, kinematic factors in the $c\bar{c}$ cross section, and the scaling of the NRQCD matrix element with the relative velocity v of the charm quark. Among those NRQCD matrix elements that scale with the minimal power of v is the one associated with the color-singlet $c\bar{c}$ channel whose angular momentum quantum numbers match those of the charmonium state H . The old *color-singlet model* for quarkonium production [2] can be defined by keeping this channel only.

If the charmonium is the only hadron in the initial or final state, the color-singlet model should be accurate up to corrections that are higher order in v . The simplest examples of such processes are electromagnetic annihilation decays, such as $J/\psi \rightarrow e^+e^-$ and $\eta_c \rightarrow \gamma\gamma$, and exclusive electromagnetic production processes, such as $\gamma\gamma \rightarrow \eta_c$. Another process for which the color-singlet model should be accurate is e^+e^- annihilation into exactly two charmonia. There are no hadrons in the initial state, and the absence of additional hadrons in the final state can be guaranteed experimentally by the monoenergetic nature of a 2-body final state. For many charmonia H , the NRQCD matrix element can be determined from the electromagnetic annihilation decay rate of either H or of another state related to H by spin symmetry. Cross sections for double-charmonium can therefore be predicted up to corrections suppressed by powers of v^2 without any unknown phenomenological factors.

One problem with e^+e^- annihilation into exclusive double charmonium is that the cross sections are very small at energies large enough to have confidence in the predictions of perturbative QCD. A naive estimate of the cross section for $J/\psi + \eta_c$ in units of the cross section for $\mu^+\mu^-$ is

$$R[J/\psi + \eta_c] \sim \alpha_s^2 \left(\frac{m_c v}{E_{\text{beam}}} \right)^6. \quad (1)$$

The 2 powers of α_s are the fewest required to produce a $c\bar{c} + c\bar{c}$ final state. There is a factor of $(m_c v)^3$ associated with the wavefunction at the origin for each charmonium. These factors in the numerator are compensated by factors of the beam energy E_{beam} in the denominator to get a dimensionless ratio. As an example, consider e^+e^- annihilation with center-of-mass energy $2E_{\text{beam}} = 10.6$ GeV. If we set $v^2 \approx 0.3$, $\alpha_s \approx 0.2$, and $m_c \approx 1.4$ GeV, we get the naive estimate $R[J/\psi + \eta_c] \approx 4 \times 10^{-7}$. This should be compared to the total ratio $R[\text{hadrons}] \approx 3.6$ for all hadronic final states [3]. The decay of the J/ψ into the easily detectable e^+e^- or $\mu^+\mu^-$ modes suppresses the observable cross section by another order of magnitude.

Fortunately, the era of high-luminosity B factories has made the measurement of such small cross sections feasible. The BABAR and BELLE detectors have each collected more than 10^7 continuum e^+e^- annihilation events and more than 10^8 events on the $\Upsilon(4S)$, 75% of which are continuum e^+e^- annihilation events. The BELLE Collaboration has recently measured the cross section for $e^+e^- \rightarrow J/\psi + \eta_c$ [4]. They also saw evidence for $J/\psi + \chi_{c0}$ and $J/\psi + \eta_c(2S)$ events.

In this paper, we calculate the cross sections for exclusive double-charmonium production via e^+e^- annihilation into a virtual photon. This process produces only charmonium states

with opposite charge conjugation. The cross sections for charmonium states with the same charge conjugation, which proceed through e^+e^- annihilation into two virtual photons, will be presented in subsequent papers [5]. We carry out the calculations in the color-singlet model including not only the diagrams of order $\alpha^2\alpha_s^2$ but also the purely electromagnetic diagrams of order α^4 , which are surprisingly large. Our result for the cross section for $J/\psi + \eta_c$ is about an order of magnitude smaller than the recent measurement by the BELLE Collaboration, although part of the discrepancy can be attributed to large relativistic corrections. The cross sections for S -wave + P -wave, P -wave + P -wave, and S -wave + D -wave charmonium states are also calculated. The cross section for $J/\psi + \eta_{c2}(1D)$ is predicted to be about a factor of 10 smaller than for $J/\psi + \eta_c$, which may be large enough for the D -wave state $\eta_{c2}(1D)$ to be discovered at the B factories.

II. COLOR-SINGLET MODEL CALCULATIONS

In this section, we use the color-singlet model to calculate the cross sections for e^+e^- annihilation through a virtual photon into a double-charmonium final state $H_1 + H_2$. Charge conjugation symmetry requires one of the charmonia to be a $C = -$ state and the other to be a $C = +$ state. The $C = -$ states with narrow widths are the $J^{PC} = 1^{--}$ states J/ψ and $\psi(2S)$, the 1^{+-} state h_c , and the yet-to-be-discovered 2^{--} state $\psi_2(1D)$. The $C = +$ states with narrow widths are the 0^{-+} states η_c and $\eta_c(2S)$, the J^{++} states $\chi_{cJ}(1P)$, $J = 0, 1, 2$, and the yet-to-be-discovered 2^{-+} state $\eta_{c2}(1D)$. We express our results in terms of the ratio $R[H_1 + H_2]$ defined by

$$R[H_1 + H_2] = \frac{\sigma[e^+e^- \rightarrow H_1 + H_2]}{\sigma[e^+e^- \rightarrow \mu^+\mu^-]}. \quad (2)$$

In the text, we give only the results for R summed over helicity states. In the Appendix, we give also the angular distribution $dR/d\cos\theta$ for each of the helicity states of H_1 and H_2 . These results may facilitate the use of partial wave analysis to resolve the experimental double-charmonium signal into contributions from the various charmonium states.

A. Asymptotic behavior

When the e^+e^- beam energy E_{beam} is much larger than the charm quark mass m_c , the relative sizes of the various double-charmonium cross sections are governed largely by the number of kinematic suppression factors r^2 , where the variable r is defined by

$$r^2 = \frac{4m_c^2}{E_{\text{beam}}^2}. \quad (3)$$

If we set $m_c = 1.4$ GeV and $E_{\text{beam}} = 5.3$ GeV, the value of this small parameter is $r^2 = 0.28$.

The asymptotic behavior of the ratio $R[H_1 + H_2]$ as $r \rightarrow 0$ can be determined from the *helicity selection rules* for exclusive processes in perturbative QCD [6, 7]. For each of the $c\bar{c}$ pairs in the final state, there is a suppression factor of r^2 due to the large momentum transfer required for the c and \bar{c} to emerge with small relative momentum. Thus, at any order in α_s , the ratio $R[H_1 + H_2]$ must decrease at least as fast as r^4 as $r \rightarrow 0$. However it may decrease more rapidly depending on the helicity states of the two hadrons. There

is of course a constraint on the possible helicities from angular momentum conservation: $|\lambda_1 - \lambda_2| = 0$ or 1 . The asymptotic behavior of the ratio $R[H_1(\lambda_1) + H_2(\lambda_2)]$ depends on the helicities λ_1 and λ_2 . The helicity selection rules imply that the slowest asymptotic decrease $R \sim r^4$ can occur only if the sum of the helicities of the hadrons is conserved. Since there are no hadrons in the initial state, hadron helicity conservation requires $\lambda_1 + \lambda_2 = 0$. The only helicity state that satisfies both this constraint and the constraint of angular momentum conservation is $(\lambda_1, \lambda_2) = (0, 0)$. For every unit of helicity by which this rule is violated, there is a further suppression factor of r^2 . The resulting estimate for the ratio R at leading order in α_s is

$$R_{\text{QCD}}[H_1(\lambda_1) + H_2(\lambda_2)] \sim \alpha_s^2 (v^2)^{3+L_1+L_2} (r^2)^{2+|\lambda_1+\lambda_2|}. \quad (4)$$

The factor of v^{3+2L} for a charmonium state with orbital angular momentum L comes from the NRQCD factors. At leading order of α_s , there may of course be further suppression factors of r^2 that arise from the simple structure of the leading-order diagrams for $e^+e^- \rightarrow c\bar{c}_1 + c\bar{c}_1$ in Fig. 1, but these suppression factors are unlikely to persist to higher orders in α_s .

The QED diagrams for $e^+e^- \rightarrow c\bar{c}_1(^3S_1) + c\bar{c}_1$ in Fig. 2 give contributions to $R[J/\psi + H_2]$ that scale in a different way with r . As $r \rightarrow 0$, the contribution to the cross section from these diagrams factors into the cross section for $\gamma + H_2$ and the fragmentation function for $\gamma \rightarrow J/\psi$. This fragmentation process produces J/ψ in a $\lambda_{J/\psi} = \pm 1$ helicity state. The hard-scattering part of the process produces only one $c\bar{c}$ pair with small relative momentum, so there is one fewer factor of r^2 relative to Eq. (4). The cross section for $\gamma + H_1$ is still subject to the helicity selection rules of perturbative QCD, so the pure QED contribution to the ratio R has the behavior

$$R_{\text{QED}}[J/\psi(\pm 1) + H_2(\lambda_2)] \sim \alpha^2 (v^2)^{3+L_2} (r^2)^{1+|\lambda_2|}. \quad (5)$$

There may also be interference terms between the QCD and QED contributions whose scaling behavior is intermediate between Eqs. (4) and (5).

B. Projections onto charmonium states

The 4 QCD diagrams for the color-singlet process $\gamma^* \rightarrow c\bar{c}_1 + c\bar{c}_1$ are shown in Fig. 1. We take the upper $c\bar{c}$ pair in Fig. 1 to form a $C = -$ charmonium H_1 with momentum P_1 and the lower $c\bar{c}$ pair to form a $C = +$ charmonium H_2 with momentum P_2 . There are also QED diagrams for $\gamma^* \rightarrow c\bar{c}_1 + c\bar{c}_1$ that can be obtained from the QCD diagrams in Fig. 1 by replacing the virtual gluons by virtual photons, but they are suppressed by a factor of α/α_s . However if one of the charmonia is a 1^{--} state like a J/ψ , there are the additional QED diagrams in Fig. 2. Although they are also suppressed by a factor of α/α_s , they are enhanced by a kinematical factor of $1/r^2$ and therefore can be more important than one might expect.

To calculate the matrix element for $e^+e^- \rightarrow H_1(P_1) + H_2(P_2)$, we start from the matrix element for $e^+e^- \rightarrow c(p_1)\bar{c}(\bar{p}_1) + c(p_2)\bar{c}(\bar{p}_2)$ with the charm quarks and antiquarks on their mass shells: $p_i^2 = \bar{p}_i^2 = m_c^2$. For each of the $c\bar{c}$ pairs, we express the momenta in the form

$$p = \frac{1}{2}P + q, \quad (6a)$$

$$\bar{p} = \frac{1}{2}P - q, \quad (6b)$$

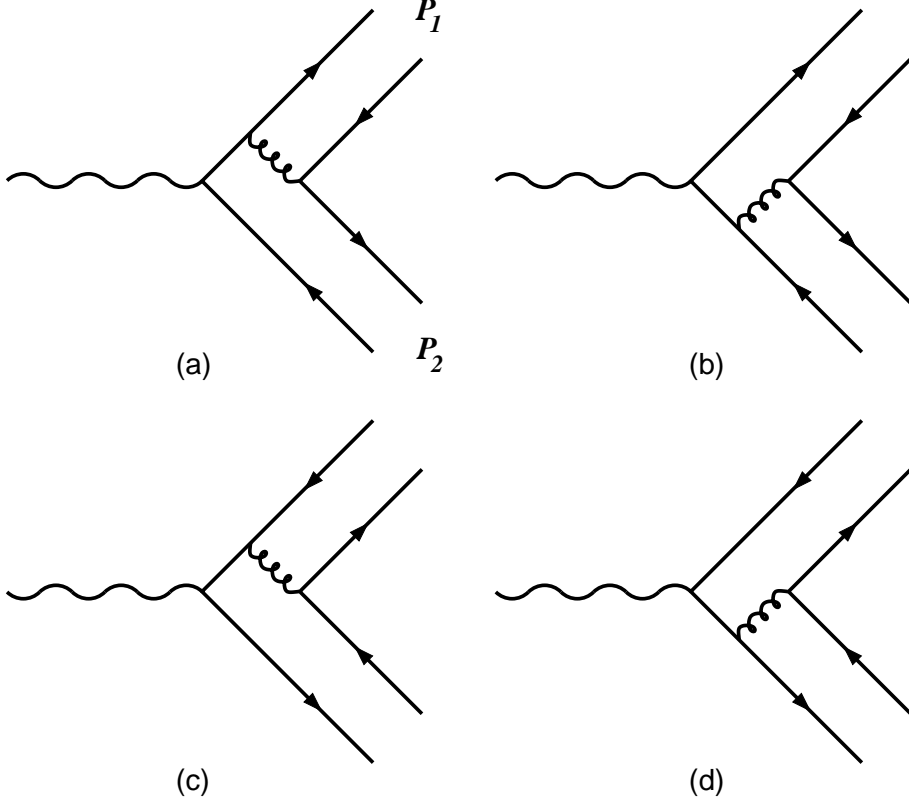


FIG. 1: QCD diagrams that can contribute to the color-singlet process $\gamma^* \rightarrow c\bar{c}_1 + c\bar{c}_1$.

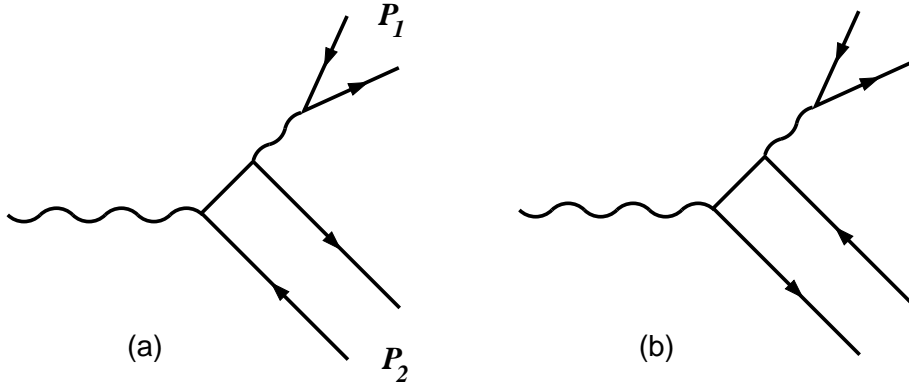


FIG. 2: QED diagrams that contribute to the color-singlet process $\gamma^* \rightarrow c\bar{c}_1 ({}^3S_1) + c\bar{c}_1$.

where P is the total momentum of the pair and q is a relative momentum that satisfies $q \cdot P = 0$. If the $c\bar{c}$ pair is in a spin-singlet color-singlet state, the matrix product of the Dirac and color spinors for the c and \bar{c} can be expressed as [9]

$$v(\bar{p})\bar{u}(p) = \frac{1}{4\sqrt{2}E(E+m_c)} (\not{p} - m_c) \gamma_5 (\not{P} + 2E) (\not{p} + m_c) \otimes \left(\frac{1}{\sqrt{N_c}} \mathbf{1} \right), \quad (7)$$

where $E^2 = P^2/4 = m_c^2 - q^2$, $N_c = 3$, and the last factor involves the unit color matrix $\mathbf{1}$. If the $c\bar{c}$ pair is in a spin-triplet color-singlet state, γ_5 in Eq. (7) is replaced by ϵ_S^* , where ϵ_S is a spin polarization vector satisfying $\epsilon_S \cdot \epsilon_S^* = -1$ and $P \cdot \epsilon_S = 0$.

In the spin-singlet case, the expansion of the matrix element in powers of q has the form

$$\mathcal{M}[c\bar{c}(S=0)] = \mathcal{A} + \mathcal{B}_\sigma q^\sigma + \mathcal{C}_{\sigma\tau} q^\sigma q^\tau + \dots \quad (8)$$

The matrix elements at leading order in v for the spin-singlet charmonium states η_c , $h_c(1P)$, and $\eta_{c2}(1D)$ can be read off from this expansion:

$$\mathcal{M}[\eta_c] = \left(\frac{\langle O_1 \rangle_{\eta_c}}{2N_c m_c} \right)^{1/2} \mathcal{A}, \quad (9a)$$

$$\mathcal{M}[h_c(\lambda)] = \left(\frac{\langle O_1 \rangle_{h_c}}{2N_c m_c^3} \right)^{1/2} \mathcal{B}_\sigma \epsilon^\sigma(\lambda), \quad (9b)$$

$$\mathcal{M}[\eta_{c2}(\lambda)] = \left(\frac{\langle O_1 \rangle_{\eta_{c2}}}{2N_c m_c^5} \right)^{1/2} \mathcal{C}_{\sigma\tau} \left[\frac{1}{2}(I^{\sigma\mu} I^{\tau\nu} + I^{\tau\mu} I^{\sigma\nu}) - \frac{1}{3} I^{\sigma\tau} I^{\mu\nu} \right] \epsilon_{\mu\nu}(\lambda), \quad (9c)$$

where $\epsilon^\tau(\lambda)$ in Eq. (9b) is a spin-1 polarization vector and $\epsilon_{\mu\nu}(\lambda)$ in Eq. (9c) is a spin-2 polarization tensor. The tensor $I_{\mu\nu}$ in Eq. (9c) is

$$I_{\mu\nu} = -g^{\mu\nu} + \frac{P^\mu P^\nu}{4m_c^2}, \quad (10)$$

where P is the expansion of $p + \bar{p}$ to leading order in q , so it now satisfies $P^2 = 4m_c^2$. The NRQCD matrix elements $\langle O_1 \rangle_{\eta_c}$ and $\langle O_1 \rangle_{h_c}$ in Eqs. (9a) and (9b) are the vacuum-saturated analogs of the NRQCD matrix elements $\langle O_1(1^1S_0) \rangle_{\eta_c}$ and $\langle O_1(1^1P_1) \rangle_{h_c}$ for annihilation decays defined in Ref. [1]. The NRQCD matrix element $\langle O_1 \rangle_{\eta_{c2}}$ in Eq. (9c) is the vacuum-saturated analog of an NRQCD matrix element $\langle O_1(1^3D_2) \rangle_{\eta_{c2}}$ which in the notation of Ref. [1] is defined by

$$\langle O_1(1^3D_2) \rangle_{\eta_{c2}} = \langle \eta_{c2} | \psi^\dagger(-\frac{i}{2})^2 \overset{\leftrightarrow}{D}^{(i)} \overset{\leftrightarrow}{D}^{(j)} \chi \chi^\dagger(-\frac{i}{2})^2 \overset{\leftrightarrow}{D}^{(i)} \overset{\leftrightarrow}{D}^{(j)} \psi | \eta_{c2} \rangle. \quad (11)$$

A projection onto the D -wave state that is equivalent to Eq. (9c) but expressed in terms of wavefunctions at the origin is given in Ref. [10].

In the spin-triplet case, the expansion of the matrix element in powers of q has the form

$$\mathcal{M}[c\bar{c}(S=1)] = (\mathcal{A}_\rho + \mathcal{B}_{\rho\sigma} q^\sigma + \mathcal{C}_{\rho\sigma\tau} q^\sigma q^\tau + \dots) \epsilon_S^\rho. \quad (12)$$

The matrix elements at leading order in v for the spin-triplet charmonium states J/ψ , $\chi_{c0}(1P)$, $\psi_1(1D)$, and $\psi_2(1D)$ can be read off from this expansion:

$$\mathcal{M}[J/\psi(\lambda)] = \left(\frac{\langle O_1 \rangle_{J/\psi}}{2N_c m_c} \right)^{1/2} \mathcal{A}_\rho \epsilon^\rho(\lambda), \quad (13a)$$

$$\mathcal{M}[\chi_{c0}] = \left(\frac{\langle O_1 \rangle_{\chi_{c0}}}{2N_c m_c^3} \right)^{1/2} \mathcal{B}_{\rho\sigma} \frac{1}{\sqrt{3}} I^{\rho\sigma}, \quad (13b)$$

$$\mathcal{M}[\chi_{c1}(\lambda)] = \left(\frac{\langle O_1 \rangle_{\chi_{c1}}}{2N_c m_c^3} \right)^{1/2} \mathcal{B}_{\rho\sigma} \frac{i}{2m_c \sqrt{2}} \epsilon^{\rho\sigma\lambda\mu} P_\lambda \epsilon_\mu(\lambda), \quad (13c)$$

$$\mathcal{M}[\chi_{c2}(\lambda)] = \left(\frac{\langle O_1 \rangle_{\chi_{c2}}}{2N_c m_c^3} \right)^{1/2} \mathcal{B}_{\rho\sigma} \left[\frac{1}{2}(I^{\rho\mu} I^{\sigma\nu} + I^{\sigma\mu} I^{\rho\nu}) - \frac{1}{3} I^{\rho\sigma} I^{\mu\nu} \right] \epsilon_{\mu\nu}(\lambda), \quad (13d)$$

$$\mathcal{M}[\psi_1(\lambda)] = \left(\frac{\langle O_1 \rangle_{\psi_1}}{2N_c m_c^5} \right)^{1/2} \mathcal{C}_{\rho\sigma\tau} \sqrt{\frac{3}{5}} \left[\frac{1}{2}(I^{\rho\sigma} I^{\tau\mu} + I^{\rho\tau} I^{\sigma\mu}) - \frac{1}{3} I^{\rho\mu} I^{\sigma\tau} \right] \epsilon_\mu(\lambda), \quad (13e)$$

$$\mathcal{M}[\psi_2(\lambda)] = \left(\frac{\langle O_1 \rangle_{\psi_2}}{2N_c m_c^5} \right)^{1/2} \mathcal{C}_{\rho\sigma\tau} \frac{i}{2m_c \sqrt{6}} [g^{\mu\sigma} \epsilon^{\tau\rho\lambda\nu} + g^{\mu\tau} \epsilon^{\sigma\rho\lambda\nu}] P_\lambda \epsilon_{\mu\nu}(\lambda). \quad (13f)$$

The NRQCD matrix elements $\langle O_1 \rangle_{J/\psi}$ and $\langle O_1 \rangle_{\chi_{cJ}}$ are the vacuum-saturated analogs of the NRQCD matrix elements $\langle O_1(^3S_1) \rangle_{J/\psi}$ and $\langle O_1(^3P_J) \rangle_{\chi_{cJ}}$ for annihilation decays defined in Ref. [1]. The NRQCD matrix elements $\langle O_1 \rangle_{\psi_1}$ and $\langle O_1 \rangle_{\psi_2}$ are the vacuum-saturated analog of the NRQCD matrix elements $\langle O_1(^3D_1) \rangle_{\psi_1}$ and $\langle O_1(^3D_2) \rangle_{\psi_2}$ which are defined by

$$\langle O_1(^3D_1) \rangle_{\psi_1} = \frac{3}{5} \langle \psi_1 | \psi^\dagger (-\frac{i}{2})^2 \sigma^i \overset{\leftrightarrow}{D}^{(i \leftrightarrow k)} \chi \chi^\dagger (-\frac{i}{2})^2 \sigma^j \overset{\leftrightarrow}{D}^{(j \leftrightarrow k)} \psi | \psi_1 \rangle, \quad (14a)$$

$$\langle O_1(^3D_2) \rangle_{\psi_2} = \frac{2}{3} \epsilon^{iab} \epsilon^{icd} \langle \psi_2 | \psi^\dagger (-\frac{i}{2})^2 \sigma^a \overset{\leftrightarrow}{D}^{(b \leftrightarrow j)} \chi \chi^\dagger (-\frac{i}{2})^2 \sigma^c \overset{\leftrightarrow}{D}^{(d \leftrightarrow j)} \psi | \psi_2 \rangle. \quad (14b)$$

C. S-wave + S-wave

The matrix element for $e^+(k_2)e^-(k_1) \rightarrow J/\psi + \eta_c$ can be written as

$$\mathcal{M} = -\frac{e_c e^2}{s} \bar{v}(k_2) \gamma^\mu u(k_1) \langle J/\psi + \eta_c | J_\mu(0) | \emptyset \rangle, \quad (15)$$

where $e_c = +\frac{2}{3}$ is the electric charge of the charm quark and $s = 4E_{\text{beam}}^2$ is the square of the center-of-mass energy. Upon simplifying the vacuum-to- $J/\psi + \eta_c$ matrix element, it reduces to the general form required by Lorentz covariance:

$$\langle J/\psi(P_1, \epsilon) + \eta_c(P_2) | J_\mu(0) | \emptyset \rangle = iA \epsilon_{\mu\nu\lambda\sigma} P_1^\nu P_2^\lambda \epsilon^\sigma, \quad (16)$$

where the coefficient A is

$$A = \frac{128\pi\alpha_s}{s^2} (\langle O_1 \rangle_{J/\psi} \langle O_1 \rangle_{\eta_c})^{1/2} \left(\frac{N_c^2 - 1}{2N_c^2} + \frac{e_c^2 \alpha}{N_c \alpha_s} + \frac{1}{r^2} \frac{e_c^2 \alpha}{\alpha_s} \right). \quad (17)$$

After squaring the amplitude and integrating over phase space, we obtain our final result for the ratio R defined in Eq. (2):

$$R[J/\psi + \eta_c] = \frac{2\pi^2\alpha_s^2}{9} X^2 (r^2 - Y)^2 r^2 (1 - r^2)^{3/2} \frac{\langle O_1 \rangle_{J/\psi} \langle O_1 \rangle_{\eta_c}}{m_c^6}, \quad (18)$$

where the coefficients X and Y are

$$X = \frac{4}{9} \left(1 + \frac{\alpha}{3\alpha_s} \right), \quad (19a)$$

$$Y = -\frac{\alpha}{\alpha_s} \left(1 + \frac{\alpha}{3\alpha_s} \right)^{-1}. \quad (19b)$$

If we set $\alpha_s = 0.21$, their numerical values are $X = 0.450$ and $Y = -0.0344$. Note that the ratio (18) depends on the charm quark mass m_c explicitly and also through the variable r defined in Eq. (3). The $\alpha^2\alpha_s^2$ term in the cross section for $e^+e^- \rightarrow J/\psi + \eta_c$ was calculated previously by Brodsky and Ji [8]. They presented their result in the form of a graph of R versus $1/r^2$, but they did not give an analytic expression for the cross section.

The only helicity states that contribute to Eq. (18) at this order in α_s are $(\lambda_1, \lambda_2) = (\pm 1, 0)$, which violate hadron helicity conservation by 1 unit. The QCD contribution to R scales like $\alpha_s^2 v^6 r^6$ in accord with Eq. (4). There is no reason to expect the amplitude for

the hadron-helicity-conserving state $(0, 0)$ to vanish at next-to-leading order in α_s , so the asymptotic behavior of the QCD contribution as $r \rightarrow 0$ is probably $R \sim \alpha_s^4 v^6 r^4$.

The pure QED contribution from the diagrams in Fig. 2 scale like $\alpha^2 v^6 r^2$ in accord with Eq. (5). The interference term is suppressed only by $\alpha/(\alpha_s r^2)$, so the QED effects are larger than one might expect. If we set $\sqrt{s} = 10.6$ GeV and $m_c = 1.4$ GeV, the electromagnetic correction increases the cross section by 29%.

The factor of $(1 - r^2)^{3/2}$ in Eq. (18) is the nonrelativistic limit of $(P_{\text{CM}}/E_{\text{beam}})^3$, where P_{CM} is the momentum of either charmonium in the center-of-momentum frame. It can be expressed as

$$\frac{P_{\text{CM}}}{E_{\text{beam}}} = \frac{\lambda^{1/2}(s, M_{H_1}^2, M_{H_2}^2)}{s}, \quad (20)$$

where $\lambda(x, y, z) = x^2 + y^2 + z^2 - 2(xy + yz + zx)$. In (18), one factor of $P_{\text{CM}}/E_{\text{beam}}$ comes from the phase space for $H_1 + H_2$, while the other two come from the square of the amplitude (16).

D. *S*-wave + *P*-wave

The ratios R for $J/\psi + \chi_{cJ}$ are

$$R[J/\psi + \chi_{cJ}] = \frac{\pi^2 \alpha_s^2}{432} X^2 F_J(r, Y) r^2 (1 - r^2)^{1/2} \frac{\langle O_1 \rangle_{J/\psi} \langle O_1 \rangle_{\chi_{cJ}}}{m_c^8}, \quad (21)$$

where the functions $F_J(r, Y)$ are

$$F_0(r, Y) = 2[4Y - 6(Y + 3)r^2 + 7r^4]^2 + r^2[4 + 2(Y + 5)r^2 - 3r^4]^2, \quad (22a)$$

$$\begin{aligned} F_1(r, Y) = & 3[8Y - 2Yr^2 + r^4]^2 + 3r^2[4Y + 2(Y + 2)r^2 - 3r^4]^2 \\ & + 3r^4[2(3Y + 4) - 7r^2]^2, \end{aligned} \quad (22b)$$

$$\begin{aligned} F_2(r, Y) = & [8Y - 6(Y + 2)r^2 + 11r^4]^2 + 2r^2[4 + 2(Y - 1)r^2 - 3r^4]^2 \\ & + 3r^2[4Y - 2(Y + 2)r^2 + 3r^4]^2 + 3r^4[2(Y + 2) - 5r^2]^2 + 6r^4[2Y - r^2]^2. \end{aligned} \quad (22c)$$

These expressions have been expressed as sums of squares of terms that correspond to the helicity amplitudes. For χ_{c0} and χ_{c2} , there are QCD contributions from all the helicity states (λ_1, λ_2) compatible with angular momentum conservation, so the leading contribution scales like $\alpha_s^2 v^8 r^4$. For χ_{c1} , there is no contribution from the hadron-helicity-conserving state $(0, 0)$, so the QCD contributions are suppressed by r^2 relative to those for χ_{c0} and χ_{c2} . The pure QED contributions to χ_{cJ} scale like $\alpha^2 v^8 r^2$ for all J in accordance with Eq. (5). The QED contribution is suppressed by a factor of $\alpha^2/(\alpha_s^2 r^2)$ for $J = 0$ and 2 but only by $\alpha^2/(\alpha_s^2 r^4)$ for $J = 1$. If we set $\sqrt{s} = 10.6$ GeV and $m_c = 1.4$ GeV, the QED corrections change the cross sections by +5.0%, -5.5%, and +11% for $J = 0, 1$, and 2, respectively.

The ratio R for $\eta_c + h_c$ is

$$R[\eta_c + h_c] = \frac{\pi^2 \alpha_s^2}{144} X^2 H(r) r^4 (1 - r^2)^{1/2} \frac{\langle O_1 \rangle_{\eta_c} \langle O_1 \rangle_{h_c}}{m_c^8}, \quad (23)$$

where the function $H(r)$ is

$$H(r) = 2r^2(r^2 - 2)^2 + (3r^4 - 6r^2 + 4)^2. \quad (24)$$

The dependence on α appears only in the overall factor X^2 because the QED contribution comes from diagrams with the same topology as the QCD diagrams in Fig. 1 of Ref. [22]. The QED contribution from the photon-fragmentation diagrams in Fig. 2 of Ref. [22] vanishes because the $+$ parity of h_c does not allow the direct coupling to a single virtual photon. The pure QCD contribution to the result in Eq. (23) is obtained by substituting $X = 4/9$. This result was first calculated correctly in Ref. [21].

E. P -wave + P -wave

The ratios R for $h_c + \chi_{cJ}$ are

$$R[h_c + \chi_{cJ}] = \frac{\pi^2 \alpha_s^2}{108} X^2 G_J(r) r^4 (1 - r^2)^{3/2} \frac{\langle O_1 \rangle_{h_c} \langle O_1 \rangle_{\chi_{cJ}}}{m_c^{10}}, \quad (25)$$

where the functions $G_J(r)$ are

$$G_0(r) = 2r^2(6 - r^2)^2, \quad (26a)$$

$$G_1(r) = 24 + 78r^2(2 - r^2)^2, \quad (26b)$$

$$G_2(r) = 3r^2(4 - 5r^2)^2 + 7r^6. \quad (26c)$$

At this order in α_s , there is no contribution to the cross sections for χ_{c0} and χ_{c2} from the helicity state $(0, 0)$, so the ratios $R[h_c + \chi_{cJ}]$ for χ_{c0} and χ_{c2} are suppressed relative to that for χ_{c1} by a factor of r^2 . The QED contribution increases the cross section by $2\alpha/(3\alpha_s) \approx 2\%$.

F. S -wave + D -wave

The ratio R for $J/\psi + \eta_{c2}$ is

$$R[J/\psi + \eta_{c2}] = \frac{4\pi^2 \alpha_s^2}{27} X^2 (Y - 2r^2)^2 r^2 (1 - r^2)^{7/2} \frac{\langle O_1 \rangle_{J/\psi} \langle O_1 \rangle_{\eta_{c2}}}{m_c^{10}}. \quad (27)$$

At this order in α_s and α , the only helicity states that contribute are $(\pm 1, 0)$. Thus the QCD contribution to the ratio R scales like $\alpha_s^2 v^{10} r^6$ in accord with Eq. (4), while the pure QED contribution scales like $\alpha^2 v^{10} r^2$ in accord with Eq. (5). If we set $\sqrt{s} = 10.6$ GeV and $m_c = 1.4$ GeV, the QED correction increases the cross section by about 15%.

The ratio R for $\psi_1 + \eta_c$ is

$$R[\psi_1 + \eta_c] = \frac{\pi^2 \alpha_s^2}{4320} X^2 (26Y - 21r^2 + 10r^4)^2 r^2 (1 - r^2)^{3/2} \frac{\langle O_1 \rangle_{\psi_1} \langle O_1 \rangle_{\eta_c}}{m_c^{10}}. \quad (28)$$

At this order in α_s and α , the only helicity states that contribute are $(\pm 1, 0)$. Thus the QCD contribution to the ratio R scales like $\alpha_s^2 v^{10} r^6$ in accord with Eq. (4), while the pure QED contribution scales like $\alpha^2 v^{10} r^2$ in accord with Eq. (5). The QED contribution increases the cross section by 41%.

The ratio R for $\psi_2 + \eta_c$ is

$$R[\psi_2 + \eta_c] = \frac{\pi^2 \alpha_s^2}{54} X^2 [6 + r^2(7 - 4r^2)^2] r^4 (1 - r^2)^{3/2} \frac{\langle O_1 \rangle_{\psi_2} \langle O_1 \rangle_{\eta_c}}{m_c^{10}}. \quad (29)$$

There is a contribution from the helicity state $(0, 0)$ that satisfies hadron helicity conservation, so the ratio R scales like r^4 in accord with Eq. (4). The QED contribution increases the cross section by $2\alpha/(3\alpha_s) \approx 2\%$.

TABLE I: The NRQCD matrix elements $\langle O_1 \rangle_H$ for the charmonium states H in units of $(\text{GeV})^{2L+3}$ where $L = 0, 1, 2$ for S -wave, P -wave, and D -wave states. The first column is the estimate from the Buchmüller-Tye potential model as given in Ref. [11]. The second and third columns are the phenomenological results from electromagnetic annihilation decays for $m_c = 1.4$ GeV at leading order (LO) and next-to-leading order (NLO) in α_s . The errors are the statistical errors associated with the experimental inputs only. The **bold-faced values** are used in the predictions for the double-charmonium cross sections.

H	potential model	phenomenology	
		LO	NLO
η_c	0.387	0.222 ± 0.024	0.297 ± 0.032
J/ψ	0.387	0.208 ± 0.015	0.335 ± 0.024
$\eta_c(2S)$	0.253		
$\psi(2S)$	0.253	0.087 ± 0.006	0.139 ± 0.010
$\chi_{c0}(1P)$	0.107	0.060 ± 0.015	0.059 ± 0.015
$\chi_{c1}(1P), h_c(1P)$	0.107		
$\chi_{c2}(1P)$	0.107	0.033 ± 0.006	0.053 ± 0.009
$\psi_1(1D)$	0.054	0.095 ± 0.015	
$\psi_2(1D), \eta_{c2}(1D)$	0.054		

III. NRQCD MATRIX ELEMENTS

The ratios R for exclusive double-charmonium production calculated in Section II depend on the NRQCD matrix elements $\langle O_1 \rangle_H$. In this section, we describe the phenomenological determination of these inputs. We also give estimates based on potential models.

A. Potential models

We can obtain estimates for the NRQCD matrix elements from the behavior of the wavefunctions near the origin in potential models. The expressions for the NRQCD matrix elements for S -wave, P -wave, and D -wave states are

$$\langle O_1 \rangle_S \approx \frac{N_c}{2\pi} |R_S(0)|^2, \quad (30a)$$

$$\langle O_1 \rangle_P \approx \frac{3N_c}{2\pi} |R'_P(0)|^2, \quad (30b)$$

$$\langle O_1 \rangle_D \approx \frac{15N_c}{4\pi} |R''_D(0)|^2. \quad (30c)$$

The values and derivatives of the radial wavefunctions at the origin for four potential models are given in Ref. [11]. Of these four potential models, the one that is most accurate at short distances is the Buchmüller-Tye potential [12]. The values of the NRQCD matrix elements for this potential are given in the first column of Table I.

B. Phenomenology

We can obtain phenomenological values for the NRQCD matrix elements $\langle O_1 \rangle_{J/\psi}$ and $\langle O_1 \rangle_{\eta_c}$ from the electronic decay rate of the J/ψ and from the photonic decay rate of the η_c [1]. The results for these decay rates, including the first QCD perturbative correction, are

$$\Gamma[\eta_c \rightarrow \gamma\gamma] = 2e_c^4 \pi \alpha^2 \frac{\langle O_1 \rangle_{\eta_c}}{m_c^2} \left(1 - \frac{20 - \pi^2}{6} \frac{\alpha_s}{\pi}\right)^2, \quad (31a)$$

$$\Gamma[J/\psi \rightarrow e^+e^-] = \frac{2e_c^2 \pi \alpha^2}{3} \frac{\langle O_1 \rangle_{J/\psi}}{m_c^2} \left(1 - \frac{8}{3} \frac{\alpha_s}{\pi}\right)^2. \quad (31b)$$

We can obtain phenomenological values for the NRQCD matrix elements $\langle O_1 \rangle_{\chi_{c0}}$ and $\langle O_1 \rangle_{\chi_{c2}}$ from the photonic decay rates of the χ_{c0} and χ_{c2} [1]. The results for these decay rates, including the first QCD perturbative correction, are

$$\Gamma[\chi_{c0} \rightarrow \gamma\gamma] = 6e_c^4 \pi \alpha^2 \frac{\langle O_1 \rangle_{\chi_{c0}}}{m_c^4} \left(1 + \frac{3\pi^2 - 28}{18} \frac{\alpha_s}{\pi}\right)^2, \quad (32a)$$

$$\Gamma[\chi_{c2} \rightarrow \gamma\gamma] = \frac{8e_c^4 \pi \alpha^2}{5} \frac{\langle O_1 \rangle_{\chi_{c2}}}{m_c^4} \left(1 - \frac{8}{3} \frac{\alpha_s}{\pi}\right)^2. \quad (32b)$$

The perturbative corrections in Eqs. (31a)–(32b) have been expressed as squares, because they can be calculated as corrections to the amplitudes. We can obtain a phenomenological value for the NRQCD matrix element $\langle O_1 \rangle_{\psi_2(1D)}$ from the electronic decay rate of the $\psi_1(1D) = \psi(3770)$, which is in the same spin-symmetry multiplet as the $\psi_2(1D)$:

$$\Gamma[\psi_1(1D) \rightarrow e^+e^-] = \frac{5e_c^2 \pi \alpha^2}{18} \frac{\langle O_1 \rangle_{\psi_1(1D)}}{m_c^6}. \quad (33)$$

The QCD perturbative correction has not been calculated.

We first determine the NRQCD matrix elements $\langle O_1 \rangle_H$ while neglecting QCD perturbative corrections. The experimental inputs are the electronic widths of the J/ψ , $\psi(2S)$, and $\psi_1(1D)$, the photonic width of the η_c , and the widths and photonic branching fractions of the χ_{c0} and χ_{c2} [13]. The only other input required is the charm quark mass m_c . The values of $\langle O_1 \rangle_H$ corresponding to $m_c = 1.4$ GeV are given in the column of Table I labelled LO. The error bars are the statistical errors associated with the experimental inputs only. To obtain $\langle O_1 \rangle_H$ for other values of m_c , we need to multiply the values in the Table by $(m_c/1.4 \text{ GeV})^{2+2L}$.

We next determine the NRQCD matrix elements $\langle O_1 \rangle_H$ including the effects of QCD perturbative corrections. We choose the QCD coupling constant to be $\alpha_s = 0.25$ corresponding to a renormalization scale of $2m_c$. The resulting values of $\langle O_1 \rangle_H$ for $m_c = 1.4$ GeV are given in the column of Table I labelled NLO. The error bars are the statistical errors associated with the experimental inputs only. To obtain $\langle O_1 \rangle_H$ for other values of m_c , we need to multiply the values in the Table by $(m_c/1.4 \text{ GeV})^{2+2L}$. Taking into account QCD perturbative corrections changes $\langle O_1 \rangle_H$ by a factor that ranges from 0.99 for χ_{c0} to 1.61 for J/ψ and χ_{c2} . The NLO values are in closer agreement with the estimates from the Buchmüller-Tye potential model than the LO values.

One complication in the determination of the NRQCD matrix element for $\psi_1(1D)$ is that this state may have substantial mixings with the $\psi(2S)$ and also with continuum $D\bar{D}$ states.

If the mixing angle between $\psi_1(1D)$ and $\psi(2S)$ is ϕ and if mixing with continuum $D\bar{D}$ states is neglected, the expressions for the electronic decay rates of the $\psi(2S)$ and $\psi_1(1D)$ are (31b) and (33) with the substitutions

$$\langle O_1 \rangle_{\psi(2S)} \longrightarrow \left| \cos \phi \langle O_1 \rangle_{2S}^{1/2} - \sin \phi \frac{\sqrt{15}}{6m_c^2} \langle O_1 \rangle_{1D}^{1/2} \right|^2, \quad (34a)$$

$$\langle O_1 \rangle_{\psi_1(1D)} \longrightarrow \left| \cos \phi \langle O_1 \rangle_{1D}^{1/2} + \sin \phi \frac{6m_c^2}{\sqrt{15}} \langle O_1 \rangle_{2S}^{1/2} \right|^2. \quad (34b)$$

A recent estimate of this effect suggests a mixing angle $\phi = 12^\circ$ [14]. The resulting values of the NRQCD matrix elements are $\langle O_1 \rangle_{2S} = 0.095$ GeV³ and $\langle O_1 \rangle_{1D} = 0.013$ GeV⁷. This value of $\langle O_1 \rangle_{1D}$ is about a factor of 7 smaller than the value of $\langle O_1 \rangle_{\psi_1(1D)}$ in Table I. Thus, if this mixing scenario is correct, the phenomenological estimate for $\langle O_1 \rangle_{\psi_2(1D)}$ in Table I could overestimate cross sections for $\psi_2(1D)$ by about a factor of 7.

Within each spin-symmetry multiplet, the NRQCD matrix elements $\langle O_1 \rangle_H$ should have differences of order v^2 which we expect to be about 30%. We choose to use the most precise phenomenological value within each spin-symmetry multiplet for all members of that multiplet. Specifically, we use the bold-faced values in the NLO column of Table I for S -wave and P -wave states and we use the bold-faced value in the LO column for the D -wave states $\eta_{c2}(1D)$, $\psi_1(1D)$, and $\psi_2(1D)$.

IV. RELATIVISTIC CORRECTIONS

In this section, we calculate the relativistic corrections to the cross sections for the S -wave double charmonium. We also give a phenomenological determination of the NRQCD factors $\langle v^2 \rangle_H$ that appear in those relativistic corrections.

A. NRQCD factor

The leading relativistic correction to the CSM amplitudes for a charmonium H are conveniently expressed in terms of a quantity that is denoted by $\langle v^2 \rangle_H$ in Ref. [1]. It can be defined formally as a ratio of matrix elements in NRQCD. For example, in the case of η_c , it can be written as

$$\langle v^2 \rangle_{\eta_c} = \frac{\langle \emptyset | \chi^\dagger (-\frac{i}{2} \mathbf{D})^2 \psi | \eta_c \rangle}{m_c^2 \langle \emptyset | \chi^\dagger \psi | \eta_c \rangle}. \quad (35)$$

The naive interpretation of $\langle v^2 \rangle_H$ is the average value of v^2 for the charm quark in the charmonium H . In the Buchmüller-Tye potential model, the average value of v^2 weighted by the probability density is 0.23 for the $1S$ states η_c and J/ψ and 0.29 for the $2S$ states $\eta_c(2S)$ and $\psi(2S)$ [12]. However the proper interpretation of the ratio of matrix elements in (35) is the average value of v^2 weighted by the wavefunction. Unfortunately this quantity has power ultraviolet divergences and requires a subtraction. For example, the wavefunction for the $1S$ states in potential models can be approximated fairly accurately by a momentum space wavefunction of the form $\psi(p) = 1/(p^2 + m_c^2 v_{1S}^2)^2$ where v_{1S} is a phenomenological parameter. The integral $\int d^3 p p^2 \psi(p)$ has a linear ultraviolet divergence. Minimal subtraction of this

linear divergence gives the negative value $\langle v^2 \rangle_H = -3v_{1S}^2$. Thus the extraction of estimates of $\langle v^2 \rangle_H$ from potential models is not straightforward.

There is a connection between the quantity $\langle v^2 \rangle_H$ and the mass of the charmonium state H that was first derived by Gremm and Kapustin [15]. The most convenient form of this relation for relativistic applications is

$$M_H^2 = 4m_c^2 (1 + \langle v^2 \rangle_H + \dots), \quad (36)$$

where the corrections are of order $m_c^2 v^4$. The mass m_c that appears in this relation is the pole mass. The pole mass suffers from renormalon ambiguities, but those ambiguities are largely compensated by corresponding ambiguities in the matrix elements that define $\langle v^2 \rangle_H$ [16, 17].

We can use the Gremm-Kapustin relation (36) to obtain a phenomenological determination of $\langle v^2 \rangle_H$ using the mass M_H of the charmonium state as input:

$$\langle v^2 \rangle_H \approx \frac{M_H^2 - 4m_c^2}{4m_c^2}. \quad (37)$$

where m_c is the pole mass of the charm quark. The masses for the charmonium states η_c , J/ψ , and $\psi(2S)$ are well-measured. The $\eta_c(2S)$ was only recently discovered by the BELLE Collaboration with a mass of $M_{\eta_c(2S)} = 3654 \pm 6 \pm 8$ MeV [18]. If we set $m_c = 1.4$ GeV, the values of $\langle v^2 \rangle_H$ for the S -wave states are $\langle v^2 \rangle_{\eta_c} = 0.13$, $\langle v^2 \rangle_{J/\psi} = 0.22$, $\langle v^2 \rangle_{\eta_c(2S)} = 0.70$, and $\langle v^2 \rangle_{\psi(2S)} = 0.73$. The values of $\langle v^2 \rangle_H$ for the $2S$ states are uncomfortably large, but those large values are necessary to compensate for the fact that $2m_c = 2.8$ GeV is far from the mass of the $2S$ states.

B. Relativistic correction factor

The relativistic correction to the cross section for the process $J/\psi + \eta_c$ can be calculated by replacing the amplitude factors (9a) and (13a) by

$$\mathcal{M}[\eta_c] = \left(\frac{M_{\eta_c} \langle O_1 \rangle_{\eta_c}}{4N_c m_c^2 (1 + \langle v^2 \rangle_{\eta_c})} \right)^{1/2} \left(\mathcal{A} + \frac{m_c^2}{3} \langle v^2 \rangle_{\eta_c} \mathcal{C}_{\sigma\tau} I^{\sigma\tau} \right), \quad (38)$$

$$\mathcal{M}[J/\psi(\lambda)] = \left(\frac{M_{J/\psi} \langle O_1 \rangle_{J/\psi}}{4N_c m_c^2 (1 + \langle v^2 \rangle_{J/\psi})} \right)^{1/2} \left(\mathcal{A}_\rho + \frac{m_c^2}{3} \langle v^2 \rangle_{J/\psi} \mathcal{C}_{\rho\sigma\tau} I^{\sigma\tau} \right) \epsilon^\rho(\lambda). \quad (39)$$

The prefactors take into account the relativistic normalizations of $c\bar{c}$ states and charmonium states. Strictly speaking, the factor of $(1 + \langle v^2 \rangle_H)^{-1/2}$ should be expanded out to first order in $\langle v^2 \rangle_H$. However if we use phenomenological determinations of the NRQCD matrix elements $\langle O_1 \rangle_H$, the prefactor in (38) or (39) cancels. We therefore choose not to expand the prefactors.

There are relativistic corrections to the electromagnetic annihilation decay rates used to determine the NRQCD matrix elements in Table I. For the decay rates of the η_c and the J/ψ given in Eqs. (31a) and (31b), the leading relativistic correction can be expressed as a multiplicative factor

$$\left(1 - \frac{1}{6} \langle v^2 \rangle_H \right)^2 \times \frac{M_H}{2m_c(1 + \langle v^2 \rangle_H)} \times \frac{2m_c}{M_H}. \quad (40)$$

The correction has been expressed as the product of three factors. The first factor, which appears squared, comes from the expansion of the amplitude in powers of the relative velocity of the $c\bar{c}$ pair. The second factor comes from the prefactor in Eq. (38) or (39). The last factor comes from the relativistic normalization factor $1/(2M_H)$ in the standard expression for the decay rate. Note that the factors of M_H cancel in Eq. (40).

We have calculated the relativistic corrections to the cross section for $J/\psi + \eta_c$. The leading correction to the ratio R in Eq. (18) can be expressed as the multiplicative factor

$$\left(1 + \frac{8Y + 3(Y + 4)r^2 - 5r^4}{12(r^2 - Y)} \langle v^2 \rangle_{J/\psi} + \frac{2Y + (Y + 14)r^2 - 5r^4}{12(r^2 - Y)} \langle v^2 \rangle_{\eta_c}\right)^2 \times \frac{M_{J/\psi}}{2m_c(1 + \langle v^2 \rangle_{J/\psi})} \frac{M_{\eta_c}}{2m_c(1 + \langle v^2 \rangle_{\eta_c})} \times \left[1 - \frac{r^2}{2(1 - r^2)} (\langle v^2 \rangle_{J/\psi} + \langle v^2 \rangle_{\eta_c})\right]^{3/2}. \quad (41)$$

The correction has been written as the product of three factors. The first factor, which appears squared, comes from the expansion of the amplitude in powers of the relative velocity of the $c\bar{c}$ pair. The second factor comes from the prefactors in Eqs. (38) and (39). The last factor is the nonrelativistic expansion of the term $(P_{\text{CM}}/E_{\text{beam}})^3$ divided by its value in the nonrelativistic limit, where one power is from the phase space factor (20) and the other two are from the square of the amplitude in Eq. (16).

Our final result for the relativistic correction can be expressed as a multiplicative factor obtained by dividing (41) by a factor of (40) for each of the charmonium states. We express it in the form:

$$\left(1 + \frac{8Y + 3(Y + 4)r^2 - 5r^4}{12(r^2 - Y)} \langle v^2 \rangle_{J/\psi} + \frac{2Y + (Y + 14)r^2 - 5r^4}{12(r^2 - Y)} \langle v^2 \rangle_{\eta_c}\right)^2 \times \left(1 - \frac{1}{6} \langle v^2 \rangle_{J/\psi}\right)^{-2} \left(1 - \frac{1}{6} \langle v^2 \rangle_{\eta_c}\right)^{-2} \times \frac{M_{J/\psi} M_{\eta_c}}{4m_c^2} \times \left(\frac{P_{\text{CM}}/E_{\text{beam}}}{(1 - r^2)^{1/2}}\right)^3. \quad (42)$$

V. PREDICTIONS FOR B FACTORIES

In this section, we calculate the cross sections for exclusive double-charmonium production in e^+e^- annihilation at the B factories. We also give a careful analysis of the errors in the predictions for $J/\psi + \eta_c$.

A. Cross sections

The results in Section II were expressed in terms of the ratio R defined in Eq. (2). The corresponding cross sections are

$$\sigma[H_1 + H_2] = \frac{4\pi\alpha^2}{3s} R[H_1 + H_2]. \quad (43)$$

The ratios R depend on a number of inputs: the coupling constants α_s and α , the charm quark mass m_c , and the NRQCD matrix elements $\langle O_1 \rangle_H$.

TABLE II: Cross sections in fb for e^+e^- annihilation into double-charmonium states $H_1 + H_2$ without relativistic corrections. The errors are only those from variations in the NLO pole mass $m_c = 1.4 \pm 0.2$ GeV.

$H_2 \setminus H_1$	J/ψ	$\psi(2S)$	$h_c(1P)$	$\psi_1(1D)$	$\psi_2(1D)$
η_c	3.78 ± 1.26	1.57 ± 0.52	0.308 ± 0.017	0.106 ± 0.025	1.04 ± 0.23
$\eta_c(2S)$	1.57 ± 0.52	0.65 ± 0.22	0.128 ± 0.007	0.044 ± 0.010	0.43 ± 0.09
$\chi_{c0}(1P)$	2.40 ± 1.02	1.00 ± 0.42	0.053 ± 0.019		
$\chi_{c1}(1P)$	0.38 ± 0.12	0.16 ± 0.05	0.258 ± 0.064		
$\chi_{c2}(1P)$	0.69 ± 0.13	0.29 ± 0.06	0.017 ± 0.002		
$\eta_{c2}(1D)$	0.35 ± 0.05	0.14 ± 0.02			

The value of the QCD coupling constant α_s depends on the choice of the scale μ . In the QCD diagrams of Fig. 1, the invariant mass of the gluon is $\sqrt{s}/2$. We therefore choose the scale to be $\mu = 5.3$ GeV. The resulting value of the QCD coupling constant is $\alpha_s(\mu) = 0.21$.

The numerical value for the pole mass m_c of the charm quark is unstable under perturbative corrections, so it must be treated with care. Since the expressions for the electromagnetic annihilation decay rates in Eqs. (31a)–(32b) include the perturbative correction of order α_s , the appropriate choice for the charm quark mass m_c in these expressions is the pole mass with corrections of order α_s included. It can be expressed as

$$m_c = \bar{m}_c(\bar{m}_c) \left(1 + \frac{4}{3} \frac{\alpha_s}{\pi} \right). \quad (44)$$

Taking the running mass of the charm quark to be $\bar{m}_c(\bar{m}_c) = 1.2 \pm 0.2$ GeV, the NLO pole mass is $m_c = 1.4 \pm 0.2$ GeV.

Our predictions for the double-charmonium cross sections without relativistic corrections are given in Table II. The error bars are those associated with the uncertainty in the NLO pole mass m_c only.

Our predictions for the double-charmonium cross sections for the S -wave states including the leading relativistic correction are obtained by multiplying the values in Table II by the factor (42). We use the values of $\langle v^2 \rangle_H$ obtained from Eq. (37), which follows from the Gremm-Kapustin relation. The resulting cross sections are given in Table III. The error bars are those associated with the uncertainty in the NLO pole mass m_c only. The relativistic corrections increase the central values of the cross sections by about 2 for $J/\psi + \eta_c$, by about 5 for $J/\psi + \eta_c(2S)$, by about 4 for $\psi(2S) + \eta_c$, and by about 8 for $\psi(2S) + \eta_c(2S)$. Although the total correction factor for $J/\psi + \eta_c$ is significantly larger than 1, it is the product of several modest correction factors that all go in the same direction. The largest individual correction factor for $J/\psi + \eta_c$ is $(1.28)^2$ coming from the expansion of the amplitude. The corresponding factors for $J/\psi + \eta_c(2S)$, $\psi(2S) + \eta_c$, and $\psi(2S) + \eta_c(2S)$ are $(1.80)^2$, $(1.64)^2$, and $(2.16)^2$, respectively. These large correction factors indicate that the relativistic corrections to the cross sections involving $2S$ states are too large to be calculated reliably using the method we have chosen.

Note that our method for calculating the relativistic correction significantly increases the sensitivity to the charm quark mass. The errors from varying m_c in Table II are about 50% for the S -wave states, while the errors in Table III correspond to increasing or decreasing the cross section by about a factor of 3. The strong sensitivity to m_c is another indication

TABLE III: Cross sections in fb for e^+e^- annihilation into S -wave double-charmonium states $H_1 + H_2$ including relativistic corrections. The errors are only those from variations in the NLO pole mass $m_c = 1.4 \pm 0.2$ GeV.

$H_2 \setminus H_1$	J/ψ	$\psi(2S)$
η_c	$7.4^{+10.9}_{-4.1}$	$6.1^{+9.5}_{-3.4}$
$\eta_c(2S)$	$7.6^{+11.8}_{-4.1}$	$5.3^{+9.1}_{-2.9}$

that our method for calculating the relativistic corrections is unreliable. We will therefore take the values in Table II to be our predictions for the cross sections and use Table III as an indication of the possible size of the relativistic corrections.

B. Perturbative corrections

The QCD perturbative corrections to the electromagnetic annihilation decay rates used to determine the NRQCD matrix elements in Table I have already been taken into account. The QCD perturbative corrections to the cross section for $J/\psi + \eta_c$ have not yet been calculated. However parts of the perturbative corrections are related to perturbative corrections that have been calculated and we can use these to estimate the order of magnitude of the perturbative corrections.

Some of the perturbative corrections can be associated with the wavefunctions of the η_c and J/ψ . For the QED diagrams in Fig. 2, the QCD perturbative corrections would be very closely related to those in the electromagnetic annihilation decay rates (31a) and (31b). However for the QCD diagrams in Fig. 1, the QCD perturbative corrections associated with the wavefunction could be very different. In the expressions for electromagnetic annihilation decay rates in Eqs. (31a)–(32b), we have 4 examples of perturbative corrections associated with wavefunctions. The root-mean-square of the 4 coefficients of α_s is 0.66. We will therefore take $(1 \pm 0.66\alpha_s)^2$ as our estimate for the perturbative correction associated with each charmonium wavefunction.

There are other perturbative corrections that can be associated with the electromagnetic charm current $\bar{c}\gamma^\mu c$. As an estimate for the magnitude of these corrections, we can use the perturbative correction to the inclusive charm cross section. The corresponding ratio R is [19]

$$R[c\bar{c} + X] = 3e_c^2(1 + r^2/8)(1 - r^2/4)^{1/2} \left[1 + \left(1 + \frac{3r^2}{4} - \frac{r^4}{16} + \dots \right) \frac{\alpha_s}{\pi} \right]. \quad (45)$$

If we set $m_c = 1.4$ GeV and $E_{\text{beam}} = 5.3$ GeV, then $r^2 = 0.28$ and the perturbative correction gives a multiplicative factor $(1 + 0.19\alpha_s)^2$.

There are also perturbative corrections that can be associated with the QCD coupling constants. We can estimate the size of these perturbative corrections by varying the scale μ up or down by a factor of 2. The factor α_s^2 in the cross section changes by a multiplicative factor of $(1 \pm 0.92\alpha_s)^2$.

To obtain an estimate of the errors in the double charmonium cross section associated with perturbative corrections, we will add in quadrature the coefficients of α_s in the perturbative correction factors associated with each wavefunction, the charm current, and the factors of

α_s . The resulting correction is a multiplicative factor $(1 \pm 1.3\alpha_s)^2$. If we set $\alpha_s = 0.21$, this factor ranges from about 0.53 to about 1.62. Thus we should not be surprised if the QCD perturbative corrections changed the predictions by 60%.

C. Color-octet contributions

According to the NRQCD factorization formalism [1], the inclusive double-charmonium cross sections are obtained by replacing the decay NRQCD matrix elements in the color-singlet model terms by production NRQCD matrix elements and by adding additional terms involving color-octet matrix elements. The color-octet contributions at this order in α_s can be obtained from the results in Section II by replacing the NRQCD matrix elements by appropriate color-octet matrix elements and by replacing the constants X and Y by the constants $X_8 = 1/\sqrt{72}$ and $Y_8 = -3$.

As an illustration, we consider the inclusive production of $J/\psi + \eta_c$. The leading color-octet contribution for $J/\psi + \eta_c + X$ can be obtained from the color-singlet model result for $\chi_{cJ} + h_c$ in Eq. (25) by substituting $\langle O_1(^3P_J) \rangle_{\chi_{cJ}} \rightarrow \langle O_8^{J/\psi}(^3P_J) \rangle / (2J+1)$, $\langle O_1(^1P_1) \rangle_{h_c} \rightarrow \langle O_8^{\eta_c}(^1P_1) \rangle$, $X \rightarrow X_8$ and $Y \rightarrow Y_8$. The ratio R for $J/\psi + \eta_c + X$ at this order includes two terms:

$$R[J/\psi + \eta_c + X] = \frac{2\pi^2\alpha_s^2}{9} X^2 (r^2 - Y)^2 r^2 (1 - r^2)^{3/2} \frac{\langle O_1^{J/\psi}(^3S_1) \rangle}{3m_c^3} \frac{\langle O_1^{\eta_c}(^1S_0) \rangle}{m_c^3} + \sum_{J=0}^2 \frac{\pi^2\alpha_s^2}{108} X_8^2 G_J(r) r^4 (1 - r^2)^{3/2} \frac{\langle O_8^{J/\psi}(^3P_J) \rangle}{(2J+1)m_c^5} \frac{\langle O_8^{\eta_c}(^1P_1) \rangle}{3m_c^5}. \quad (46)$$

By the velocity-scaling rules of NRQCD [1], the color-octet term is suppressed by a power of v^8 , but that is partly compensated by an enhancement factor of $1/r^6$. Omitting the color-octet term and applying the vacuum-saturation approximation to the NRQCD matrix elements in the color-singlet term, we recover the nonrelativistic limit of the ratio R in Eq. (18) for the exclusive $J/\psi + \eta_c$ final state.

Color-octet processes can also contribute to the exclusive cross section for $J/\psi + \eta_c$. The 2 gluons emitted by one color-octet $c\bar{c}$ pair in the transition to a color-singlet state that can form charmonium can be absorbed by the other color-octet $c\bar{c}$ pair. The amplitude is suppressed by v^4 relative to the color-singlet amplitude. The leading contribution to the cross section will come from the interference between these two amplitudes and so will be suppressed only by v^4 . The interference terms cancel when summed over all possible final states, so they do not appear in the inclusive cross section (46). The color-octet contributions will also have suppression factors of r^2 that guarantee consistency with the helicity selection rules of perturbative QCD in the limit $r \rightarrow 0$.

D. Phenomenology

The BELLE Collaboration has recently measured the cross section for $J/\psi + \eta_c$ [4]. The J/ψ was detected through its decays into $\mu^+\mu^-$ and e^+e^- , which have a combined branching fraction of about 12%. The η_c was observed as a peak in the momentum spectrum of the J/ψ corresponding to the 2-body process $J/\psi + \eta_c$. The measured cross section is

$$\sigma[J/\psi + \eta_c] \times B[\geq 4] = (33^{+7}_{-6} \pm 9) \text{ fb}, \quad (47)$$

where $B[\geq 4]$ is the branching fraction for the η_c to decay into at least 4 charged particles. Since $B[\geq 4] < 1$, the right side of Eq. (47) is a lower bound on the cross section for $J/\psi + \eta_c$.

The lower bound provided by Eq. (47) is about an order of magnitude larger than the central value 3.8 fb of the calculated cross section for $J/\psi + \eta_c$ in Table II. The largest theoretical errors are QCD perturbative corrections, which we estimate to give an uncertainty of roughly 60%, the value of m_c , which we estimate to give an uncertainty of roughly 50%, and a relativistic correction that we have not been able to quantify with confidence. If we take the calculations of the relativistic corrections in Table III seriously, the extreme upper end of the prediction is marginally compatible with the BELLE measurement. In our further discussion, we will ignore the large discrepancy between the predicted cross section for $J/\psi + \eta_c$ and the BELLE measurement. We will focus on predictions for the ratios of cross sections from Table II under the assumption that many of the theoretical errors will cancel in the ratio.

In addition to measuring the cross section for $J/\psi + \eta_c$, the BELLE Collaboration saw evidence for $J/\psi + \eta_c(2S)$ and $J/\psi + \chi_{c0}(1P)$ [4] events. A 3-peak fit to the momentum spectrum of the J/ψ gave approximately 67, 42, and 39 events for η_c , $\eta_c(2S)$, and $\chi_{c0}(1P)$ with fluctuations of 12-15 events. The proportion of $J/\psi + \eta_c$, $J/\psi + \eta_c(2S)$, and $J/\psi + \chi_{c0}(1P)$ events, $1.00 : 0.63 \pm 0.25 : 0.58 \pm 0.24$, is consistent with the proportions $1.00 : 0.41 : 0.63$ of the cross sections in Table II. These proportions are insensitive to the choice of m_c . The absence of peaks corresponding to $\chi_{c1}(1P)$ and $\chi_{c2}(1P)$ is also consistent with Table II. The cross sections for $J/\psi + \chi_{cJ}(1P)$ for $J = 1$ and 2 are predicted to be smaller than for $J = 0$ by factors of about 0.16 and 0.29, respectively.

If the cross sections for the narrow D -wave states are large enough, they could be discovered at the B factories. The state $\eta_{c2}(1D)$ could be observed as a peak in the momentum spectrum of J/ψ corresponding to the 2-body process $J/\psi + \eta_{c2}(1D)$. The prediction in Table II for the cross section for $J/\psi + \eta_{c2}(1D)$ is smaller than that for $J/\psi + \eta_c$ by about a factor 0.09. It might also be possible to discover the D -wave state $\psi_2(1D)$ as a peak in the momentum spectrum of η_c corresponding to the 2-body process $\psi_2(1D) + \eta_c$. The η_c could be detected through its decay into $KK\pi$, whose branching fraction is about 6%. The prediction in Table II for the cross section for $\psi_2(1D) + \eta_c$ is smaller than that for $J/\psi + \eta_c$ only by about a factor 0.27. Our predictions for the cross sections for $J/\psi + \eta_{c2}(1D)$ and $\psi_2(1D) + \eta_c$ are based on a phenomenological determination of the NRQCD matrix elements that ignored mixing between the $\psi(2S)$ and the $\psi_1(1D)$. If there is significant mixing between these two states, the cross sections for S -wave + D -wave could be a factor of 7 smaller.

In summary, we have calculated the cross sections for e^+e^- annihilation into exclusive double charmonium states with opposite charge conjugation. Many of the cross sections are large enough to be observed at B factories. In particular, it may be possible to discover the D -wave states $\eta_{c2}(1D)$ and $\psi_2(1D)$. The cross sections for double charmonium suffer from fewer theoretical uncertainties than inclusive charmonium cross sections. The largest uncertainty comes from relativistic corrections. Measurements of exclusive double charmonium cross sections will provide strong motivation for developing reliable methods for calculating the relativistic corrections to quarkonium cross sections.

Note added: Liu, He, and Chao have calculated the $\alpha^2\alpha_s^2$ terms in the cross sections for e^+e^- annihilation into $J/\psi + H$, $H = \eta_c, \chi_{c0}, \chi_{c1}, \chi_{c2}$ [20]. Their results are consistent with ours. In Ref. [21], Liu, He, and Chao calculated the $\alpha^2\alpha_s^2$ terms in the differential cross sections for $J/\psi + \eta_c$, $J/\psi + \chi_{c0}$, and $\eta_c + h_c$. Their results for $J/\psi + \eta_c$ and $J/\psi + \chi_{c0}$ agree

with ours. Our corrected result for $\eta_c + h_c$ in Eq. (23) agrees with their result.

APPENDIX A: ANGULAR DISTRIBUTIONS

In this appendix, we give the angular distributions dR/dx for $e^+e^- \rightarrow H_1(\lambda_1) + H_2(\lambda_2)$ for each of the helicity states that contribute at order $\alpha^2\alpha_s^2$ or α^4 . The angular variable is $x = \cos\theta$, where θ is the angle between e^- and H_1 in the e^+e^- center-of-mass frame. The results for R in the text are obtained by summing over all the helicities and integrating over $-1 < x < +1$.

1. *S*-wave + *S*-wave

The angular distribution for $J/\psi + \eta_c$ is

$$\frac{dR}{dx}[J/\psi(\pm 1) + \eta_c] = \frac{\pi^2\alpha_s^2}{24} X^2(r^2 - Y)^2 r^2 (1 - r^2)^{3/2} \frac{\langle O_1 \rangle_{J/\psi} \langle O_1 \rangle_{\eta_c}}{m_c^6} (1 + x^2), \quad (\text{A1})$$

The cross section for the longitudinal helicity component $\lambda_1 = 0$ of the J/ψ vanishes.

2. *S*-wave + *P*-wave

The angular distributions for $J/\psi + \chi_{cJ}$ are

$$\frac{dR}{dx}[J/\psi(\lambda_1) + \chi_{cJ}(\lambda_2)] = \frac{\pi^2\alpha_s^2}{432} X^2 r^2 (1 - r^2)^{1/2} \frac{\langle O_1 \rangle_{J/\psi} \langle O_1 \rangle_{\chi_{cJ}}}{m_c^8} F_J(\lambda_1, \lambda_2, x). \quad (\text{A2})$$

The non-vanishing entries of $F_J(\lambda_1, \lambda_2, x)$ are

$$F_0(0, 0, x) = \frac{3}{4} r^2 [4 + 2(Y + 5)r^2 - 3r^4]^2 (1 - x^2), \quad (\text{A3a})$$

$$F_0(\pm 1, 0, x) = \frac{3}{8} [4Y - 6(Y + 3)r^2 + 7r^4]^2 (1 + x^2), \quad (\text{A3b})$$

$$F_1(0, \pm 1, x) = \frac{9}{16} r^4 [2(3Y + 4) - 7r^2]^2 (1 + x^2), \quad (\text{A3c})$$

$$F_1(\pm 1, 0, x) = \frac{9}{16} [8Y - 2Yr^2 + r^4]^2 (1 + x^2), \quad (\text{A3d})$$

$$F_1(\pm 1, \pm 1, x) = \frac{9}{8} r^2 [4Y + 2(Y + 2)r^2 - 3r^4]^2 (1 - x^2), \quad (\text{A3e})$$

$$F_2(0, 0, x) = \frac{3}{2} r^2 [4 + 2(Y - 1)r^2 - 3r^4]^2 (1 - x^2), \quad (\text{A3f})$$

$$F_2(0, \pm 1, x) = \frac{9}{16} r^4 [2(Y + 2) - 5r^2]^2 (1 + x^2), \quad (\text{A3g})$$

$$F_2(\pm 1, 0, x) = \frac{3}{16} [8Y - 6(Y + 2)r^2 + 11r^4]^2 (1 + x^2), \quad (\text{A3h})$$

$$F_2(\pm 1, \pm 1, x) = \frac{9}{8} r^2 [4Y - 2(Y + 2)r^2 + 3r^4]^2 (1 - x^2), \quad (\text{A3i})$$

$$F_2(\pm 1, \pm 2, x) = \frac{9}{8} r^4 [2Y - r^2]^2 (1 + x^2). \quad (\text{A3j})$$

The angular distribution for $\eta_c + h_c$ is

$$\frac{dR}{dx} [\eta_c + h_c(\lambda)] = \frac{\pi^2 \alpha_s^2}{144} X^2 r^4 (1 - r^2)^{1/2} \frac{\langle O_1 \rangle_{\eta_c} \langle O_1 \rangle_{h_c}}{m_c^8} H(\lambda, x), \quad (\text{A4})$$

where

$$H(0, x) = \frac{3}{4} (1 - x^2) (3r^4 - 6r^2 + 4)^2, \quad (\text{A5a})$$

$$H(\pm 1, x) = \frac{3}{8} (1 + x^2) r^2 (r^2 - 2)^2. \quad (\text{A5b})$$

3. *P-wave + P-wave*

The angular distributions for $h_c + \chi_{cJ}$ are

$$\frac{dR}{dx} [h_c(\lambda_1) + \chi_{cJ}(\lambda_2)] = \frac{\pi^2 \alpha_s^2}{108} X^2 r^4 (1 - r^2)^{3/2} \frac{\langle O_1 \rangle_{h_c} \langle O_1 \rangle_{\chi_{cJ}}}{m_c^{10}} G_J(\lambda_1, \lambda_2, x). \quad (\text{A6})$$

where non-vanishing entries of $G_J(\lambda_1, \lambda_2, x)$ are given by

$$G_0(\pm 1, 0, x) = \frac{3}{8} r^2 (6 - r^2)^2 (1 + x^2), \quad (\text{A7a})$$

$$G_1(0, 0, x) = 18 (1 - x^2), \quad (\text{A7b})$$

$$G_1(0, \pm 1, x) = \frac{225}{16} r^2 (2 - r^2)^2 (1 + x^2), \quad (\text{A7c})$$

$$G_1(\pm 1, 0, x) = \frac{9}{16} r^2 (2 - r^2)^2 (1 + x^2), \quad (\text{A7d})$$

$$G_2(0, \pm 1, x) = \frac{9}{16} r^2 (4 - 5r^2)^2 (1 + x^2), \quad (\text{A7e})$$

$$G_2(\pm 1, 0, x) = \frac{3}{16} r^6 (1 + x^2), \quad (\text{A7f})$$

$$G_2(\pm 1, \pm 2, x) = \frac{9}{8} r^6 (1 + x^2). \quad (\text{A7g})$$

Note that $G_2(\pm 1, 0, x)$ is more suppressed than the prediction from the hadron helicity conservation rule.

4. *S-wave + D-wave*

The angular distributions for $J/\psi + \eta_{c2}$ are

$$\frac{dR}{dx} [J/\psi(\pm 1) + \eta_{c2}(0)] = \frac{\pi^2 \alpha_s^2}{36} X^2 (Y - 2r^2)^2 r^2 (1 - r^2)^{7/2} \frac{\langle O_1 \rangle_{J/\psi} \langle O_1 \rangle_{\eta_{c2}}}{m_c^{10}} (1 + x^2). \quad (\text{A8})$$

The cross sections for the longitudinal helicity component $\lambda_1 = 0$ of the J/ψ and the helicity components $\lambda_2 = \pm 1$ and ± 2 of the η_{c2} vanish.

The angular distributions for $\psi_1 + \eta_c$ are

$$\frac{dR}{dx}[\psi_1(\pm 1) + \eta_c] = \frac{\pi^2 \alpha_s^2}{23040} X^2 (26Y - 21r^2 + 10r^4)^2 r^2 (1 - r^2)^{3/2} \frac{\langle O_1 \rangle_{\psi_1} \langle O_1 \rangle_{\eta_c}}{m_c^{10}} (1 + x^2). \quad (\text{A9})$$

The cross section for the longitudinal helicity component $\lambda_1 = 0$ of the ψ_1 vanishes.

The angular distributions for $\psi_2 + \eta_c$ are

$$\frac{dR}{dx}[\psi_2(\lambda_1) + \eta_c] = \frac{\pi^2 \alpha_s^2}{54} X^2 r^4 (1 - r^2)^{3/2} \frac{\langle O_1 \rangle_{\psi_2} \langle O_1 \rangle_{\eta_c}}{m_c^{10}} H(\lambda_1, x). \quad (\text{A10})$$

The non-vanishing entries of $H(\lambda_1, x)$ are

$$H(0, x) = \frac{9}{2} (1 - x^2), \quad (\text{A11a})$$

$$H(\pm 1, x) = \frac{3}{16} r^2 (7 - 4r^2)^2 (1 + x^2). \quad (\text{A11b})$$

ACKNOWLEDGMENTS

We thank G. T. Bodwin and E. Eichten for many useful discussions. We acknowledge B. Yabsley for a suggestion that led to our adding the Appendix. We thank Chaehyun Yu for his help in checking some of the calculations. The research of E.B. is supported in part by the U. S. Department of Energy, Division of High Energy Physics, under grant DE-FG02-91-ER4069 and by Fermilab, which is operated by Universities Research Association Inc. under Contract DE-AC02-76CH03000 with the U. S. Department of Energy. The research of J.L. in the High Energy Physics Division at Argonne National Laboratory is supported by the U. S. Department of Energy, Division of High Energy Physics, under Contract W-31-109-ENG-38.

[1] G. T. Bodwin, E. Braaten, and G. P. Lepage, Phys. Rev. D **51**, 1125 (1995) [Erratum-ibid. D **55**, 5853 (1997)] [arXiv:hep-ph/9407339].

[2] M. B. Einhorn and S. D. Ellis, Phys. Rev. D **12**, 2007 (1975); S. D. Ellis, M. B. Einhorn, and C. Quigg, Phys. Rev. Lett. **36**, 1263 (1976); C. E. Carlson and R. Suaya, Phys. Rev. D **14**, 3115 (1976); J. H. Kühn, Phys. Lett. B **89**, 385 (1980); T. A. DeGrand and D. Toussaint, Phys. Lett. B **89**, 256 (1980); J. H. Kühn, S. Nussinov, and R. Rückl, Z. Phys. C **5**, 117 (1980); M. B. Wise, Phys. Lett. B **89**, 229 (1980); C. H. Chang, Nucl. Phys. B **172**, 425 (1980); R. Baier and R. Rückl, Phys. Lett. B **102**, 364 (1981); E. L. Berger and D. Jones, Phys. Rev. D **23**, 1521 (1981); W. Y. Keung, in *The Cornell Z⁰ Theory Workshop*, edited by M. E. Peskin and S.-H. Tye (Cornell University, Ithaca, 1981).

[3] R. Ammar *et al.* [CLEO Collaboration], Phys. Rev. D **57**, 1350 (1998) [arXiv:hep-ex/9707018].

[4] K. Abe *et al.* [BELLE Collaboration], Phys. Rev. Lett. **89**, 142001 (2002) [arXiv:hep-ex/0205104].

[5] G. T. Bodwin, J. Lee, and E. Braaten, arXiv:hep-ph/0212181; arXiv:hep-ph/0212352.

[6] V. L. Chernyak and A. R. Zhitnitsky, Sov. J. Nucl. Phys. **31** (1980) 544 [Yad. Fiz. **31** (1980) 1053].

- [7] S. J. Brodsky and G. P. Lepage, Phys. Rev. D **24**, 2848 (1981).
- [8] S. J. Brodsky and C.-R. Ji, Phys. Rev. Lett. **55**, 2257 (1985).
- [9] G. T. Bodwin and A. Petrelli, Phys. Rev. D **66**, 094011 (2002) [arXiv:hep-ph/0205210].
- [10] L. Bergström, H. Grotch, and R. W. Robinett, Phys. Rev. D **43**, 2157 (1991).
- [11] E. J. Eichten and C. Quigg, Phys. Rev. D **52**, 1726 (1995) [arXiv:hep-ph/9503356].
- [12] W. Buchmüller and S.-H. H. Tye, Phys. Rev. D **24**, 132 (1981).
- [13] K. Hagiwara *et al.* [Particle Data Group Collaboration], Phys. Rev. D **66**, 010001 (2002).
- [14] J. L. Rosner, Phys. Rev. D **64**, 094002 (2001) [arXiv:hep-ph/0105327].
- [15] M. Gremm and A. Kapustin, Phys. Lett. B **407**, 323 (1997) [arXiv:hep-ph/9701353].
- [16] E. Braaten and Y.-Q. Chen, Phys. Rev. D **57**, 4236 (1998) [Erratum-ibid. D **59**, 079901 (1999)] [arXiv:hep-ph/9710357].
- [17] G. T. Bodwin and Y.-Q. Chen, Phys. Rev. D **60**, 054008 (1999) [arXiv:hep-ph/9807492].
- [18] S. K. Choi *et al.* [BELLE Collaboration], Phys. Rev. Lett. **89**, 102001 (2002) [Erratum-ibid. **89**, 129901 (2002)] [arXiv:hep-ex/0206002].
- [19] K. G. Chetyrkin and J. H. Kühn, Phys. Lett. B **342**, 356 (1995) [arXiv:hep-ph/9409444].
- [20] K. Y. Liu, Z. G. He and K. T. Chao, Phys. Lett. B **557**, 45 (2003) [arXiv:hep-ph/0211181].
- [21] K. Y. Liu, Z. G. He and K. T. Chao, arXiv:hep-ph/0408141.
- [22] E. Braaten and J. Lee, Phys. Rev. D **67**, 054007 (2003) [arXiv:hep-ph/0211085].

**Erratum: Exclusive double-charmonium production
from e^+e^- annihilation into a virtual photon
[Phys. Rev. D 67, 054007 (2003)]**

Eric Braaten

Physics Department, Ohio State University, Columbus, Ohio 43210, USA

Jungil Lee

Department of Physics, Korea University, Seoul 136-701, Korea

In Ref. [1], we calculated the cross sections for exclusive double-charmonium production from e^+e^- annihilation into a virtual photon. We made an error in the calculation by omitting a relative minus sign between diagrams that differ by the interchange of identical fermions in the final state. That error was also made in Refs. [2] and [3]. In Ref. [1], the error was the omission of a relative minus sign between the sum of the four Feynman diagrams in Fig. 1 and the sum of the two QED Feynman diagrams in Fig. 2. We also made a separate error in the calculation of the cross section for $\eta_c + h_c$. We show corrections in boldface type, except in display equations.

The expression in Eq. (17) for the coefficient A in the amplitude for $J/\psi + \eta_c$ should be corrected as follows:

$$A = \frac{128\pi\alpha_s}{s^2} (\langle O_1 \rangle_{J/\psi} \langle O_1 \rangle_{\eta_c})^{1/2} \left(\frac{N_c^2 - 1}{2N_c^2} + \frac{e_c^2 \alpha}{N_c \alpha_s} + \frac{1}{r^2} \frac{e_c^2 \alpha}{\alpha_s} \right). \quad (17)$$

The sign in front of $1/r^2$ term has been reversed. In the expression for the coefficient Y in Eq. (19b), the overall sign should also be reversed:

$$Y = -\frac{\alpha}{\alpha_s} \left(1 + \frac{\alpha}{3\alpha_s} \right)^{-1}. \quad (19b)$$

In the subsequent sentence, the numerical value of Y should have the opposite sign: $Y = -0.0344$.

In Section II, the descriptions for the changes in various cross sections due to the QED contribution should be corrected as follows:

- Sec. II C (S-wave + S-wave) above Eq. (20): If we set $\sqrt{s} = 10.6$ GeV and $m_c = 1.4$ GeV, the electromagnetic correction **increases** the cross section by **29%**.
- Sec. II D (S-wave + P-wave) above Eq. (23): If we set $\sqrt{s} = 10.6$ GeV and $m_c = 1.4$ GeV, the QED corrections change the cross sections by **+5.0%**, **-5.5%**, and **+11%** for $J = 0, 1$, and 2 , respectively.
- Sec. II F (S-wave + D-wave) below Eq. (26): If we set $\sqrt{s} = 10.6$ GeV and $m_c = 1.4$ GeV, the QED correction **increases** the cross section by about **15%**.
- Sec. II F (S-wave + D-wave) below Eq. (27): The QED contribution increases the cross section by **41%**.

There are several corrections to the text in Section V:

- The relativistic corrections increase the central values of the cross sections by about **2** for $J/\psi + \eta_c$, by about **5** for $J/\psi + \eta_c(2S)$, by about **4** for $\psi(2S) + \eta_c$, and by about **8** for $\psi(2S) + \eta_c(2S)$.
- The largest individual correction factor for $J/\psi + \eta_c$ is **(1.28)²** coming from the expansion of the amplitude. The corresponding factors for $J/\psi + \eta_c(2S)$, $\psi(2S) + \eta_c$, and $\psi(2S) + \eta_c(2S)$ are **(1.80)²**, **(1.64)²**, and **(2.16)²**, respectively.
- The lower bound provided by Eq. (46) is about an order of magnitude larger than the central value **3.8** fb of the calculated cross section for $J/\psi + \eta_c$ in Table II.
- The proportion of [$J/\psi + \eta_c$, $J/\psi + \eta_c(2S)$, and $J/\psi + \chi_{c0}(1P)$ events,] $1.00 : 0.63 \pm 0.25 : 0.58 \pm 0.24$, is **consistent** with the proportions $1.00 : 0.41 : 0.63$ of the cross sections in Table II.
- The cross sections for $J/\psi + \chi_{cJ}(1P)$ for $J = 1$ and 2 are predicted to be smaller than for $J = 0$ by factors of about **0.16** and **0.29**, respectively.

TABLE II: Cross sections in fb for e^+e^- annihilation into double-charmonium states $H_1 + H_2$ without relativistic corrections. The errors are only those from variations in the NLO pole mass $m_c = 1.4 \pm 0.2$ GeV.

$H_2 \setminus H_1$	J/ψ	$\psi(2S)$	$h_c(1P)$	$\psi_1(1D)$	$\psi_2(1D)$
η_c	3.78 ± 1.26	1.57 ± 0.52	0.308 ± 0.017	0.106 ± 0.025	1.04 ± 0.23
$\eta_c(2S)$	1.57 ± 0.52	0.65 ± 0.22	0.128 ± 0.007	0.044 ± 0.010	0.43 ± 0.09
$\chi_{c0}(1P)$	2.40 ± 1.02	1.00 ± 0.42	0.053 ± 0.019		
$\chi_{c1}(1P)$	0.38 ± 0.12	0.16 ± 0.05	0.258 ± 0.064		
$\chi_{c2}(1P)$	0.69 ± 0.13	0.29 ± 0.06	0.017 ± 0.002		
$\eta_{c2}(1D)$	0.35 ± 0.05	0.14 ± 0.02			

TABLE III: Cross sections in fb for e^+e^- annihilation into S -wave double-charmonium states $H_1 + H_2$ including relativistic corrections. The errors are only those from variations in the NLO pole mass $m_c = 1.4 \pm 0.2$ GeV.

$H_2 \setminus H_1$	J/ψ	$\psi(2S)$
η_c	$7.4^{+10.9}_{-4.1}$	$6.1^{+9.5}_{-3.4}$
$\eta_c(2S)$	$7.6^{+11.8}_{-4.1}$	$5.3^{+9.1}_{-2.9}$

- The prediction in Table II for the cross section for $J/\psi + \eta_{c2}(1D)$ is smaller than that for $J/\psi + \eta_c$ by about a factor **0.09**.
- The prediction in Table II for the cross section for $\psi_2(1D) + \eta_c$ is smaller than that for $J/\psi + \eta_c$ only by about a factor **0.27**.

In Ref. [1], we also made an error in the calculation of the cross section for $\eta_c + h_c$. The result that was obtained for the ratio R in Eq. (23) was zero. The correct result is

$$R[\eta_c + h_c] = \frac{\pi^2 \alpha_s^2}{144} X^2 H(r) r^4 (1 - r^2)^{1/2} \frac{\langle O_1 \rangle_{\eta_c} \langle O_1 \rangle_{h_c}}{m_c^8}, \quad (23)$$

where the function $H(r)$ is

$$H(r) = 2r^2(r^2 - 2)^2 + (3r^4 - 6r^2 + 4)^2.$$

The dependence on α appears only in the overall factor X^2 because the QED contribution comes from diagrams with the same topology as the QCD diagrams in Fig. 1 of Ref. [1]. The QED contribution from the photon-fragmentation diagrams in Fig. 2 of Ref. [1] vanishes because the $+$ parity of h_c does not allow the direct coupling to a single virtual photon. The pure QCD contribution to the result in Eq. (23) is obtained by substituting $X = 4/9$. This result was first calculated correctly in Ref. [4]. The angular distribution for $\eta_c + h_c$ is

$$\frac{dR}{dx} [\eta_c + h_c(\lambda)] = \frac{\pi^2 \alpha_s^2}{144} X^2 r^4 (1 - r^2)^{1/2} \frac{\langle O_1 \rangle_{\eta_c} \langle O_1 \rangle_{h_c}}{m_c^8} H(\lambda, x),$$

where

$$\begin{aligned} H(0, x) &= \frac{3}{4} (1 - x^2) (3r^4 - 6r^2 + 4)^2, \\ H(\pm 1, x) &= \frac{3}{8} (1 + x^2) r^2 (r^2 - 2)^2. \end{aligned}$$

The error in the calculations produced errors in the numerical predictions for some of the cross sections given in Tables II and III of Ref. [1]. Those Table are reproduced here, with the corrected values given in boldface.

We thank Chaehyun Yu for his help in checking some of the calculations.

[1] E. Braaten and J. Lee, Phys. Rev. D **67**, 054007 (2003) [arXiv:hep-ph/0211085].
[2] G. T. Bodwin, J. Lee and E. Braaten, Phys. Rev. Lett. **90**, 162001 (2003) [arXiv:hep-ph/0212181].
[3] G. T. Bodwin, J. Lee and E. Braaten, Phys. Rev. D **67**, 054023 (2003) [arXiv:hep-ph/0212352].
[4] K. Y. Liu, Z. G. He and K. T. Chao, arXiv:hep-ph/0408141.